Contrasting glacier variations of Glaciar Perito Moreno and Glaciar Ameghino, Southern Patagonia Icefield

Masahiro MINOWA,[1,2] Shin SUGIYAMA,[1] Daiki SAKAKIBARA,[1,2] Takanobu SAWAGAKI[3]

[1]*Institute of Low Temperature Science, Hokkaido University, Sapporo, Japan*
[2]*Graduate School of Environmental Science, Hokkaido University, Sapporo, Japan*
[3]*Faculty of Environmental Earth Science, Hokkaido University, Sapporo, Japan*
Correspondence: Masahiro Minowa <m_masa@lowtem.hokudai.ac.jp>

ABSTRACT. Glaciar Perito Moreno (GPM) and Glaciar Ameghino (GA), Southern Patagonia Icefield, are in contact in the accumulation area, but have shown contrasting frontal variations in the past few decades. To investigate recent changes of the two glaciers and processes controlling the different responses to similar climate conditions, we measured surface elevation change from 2000 to 2008 and terminus positions from 1999 to 2012 using several types of satellite data. GPM shows no significant changes in terminus position and $0.4 \pm 0.3\,\mathrm{m\,a^{-1}}$ thickening over the period, whereas GA retreated $55 \pm 2\,\mathrm{m\,a^{-1}}$ and thinned $2.6 \pm 0.3\,\mathrm{m\,a^{-1}}$. Mass-balance measurements over the period 1999/2000 show that accumulation at GPM was ten times greater than that at GA, but ablation was only three times greater. The mass-balance–altitude profile is similar for the two glaciers; differences in the mass-balance distribution are caused by differences in the accumulation–area ratio (AAR). Our results suggest that the AAR and the calving flux exert strong control on the evolution of glaciers in the region.

KEYWORDS: calving, glacier fluctuations, glacier mass balance, remote sensing

1. INTRODUCTION

The Northern Patagonia Icefield (3976 $\mathrm{km^2}$; Davies and Glasser, 2012) and the Southern Patagonia Icefield (SPI) (12 550 $\mathrm{km^2}$; Skvarca and others, 2010) form the largest temperate mountain glacier system in the Southern Hemisphere. Of the 69 major outlet glaciers in the region, 62 calve into lakes and the ocean (Aniya, 1999). Previous studies show that most major calving glaciers in Patagonia have been retreating over the past few decades (Aniya and others, 1997; Masiokas and others, 2009; Lopez and others, 2010; Willis and others, 2012; Sakakibara and Sugiyama, 2014). As a consequence, the icefields have been losing ice mass and contributing to the sea-level rise (e.g. Rignot and others, 2003; Rivera and others, 2007; Willis and others, 2012).

Recent glacier variations in Patagonia are not uniform (Sakakibara and Sugiyama, 2014). For example, Glaciar Upsala has been retreating and thinning since 2008 at rates significantly greater than those of other glaciers (Muto and Furuya, 2013; Sakakibara and Sugiyama, 2014). Glaciar Jorge Montt also rapidly retreated and thinned in the 1990s and 2009–11 (Rivera and others, 2012). On the other hand, other calving glaciers have been stable or have advanced over the past few decades. For example, Glaciar Pío XI has advanced by >1000 m since the beginning of the 20th century (Aniya and others, 1997). Glaciar Perito Moreno (GPM) also advanced at the beginning of the 20th century but has only shown small fluctuations (±500 m) since 1920 (Skvarca and Naruse, 1997). The observations indicate that calving glacier variations in Patagonia are not controlled by climate alone as demonstrated by previous studies in other regions (Meier and Post, 1987; Benn and others, 2007; Post and others, 2011).

Changes in surface mass balance forced by climate have caused the recent retreat of calving glaciers in Patagonia, but the sensitivity to climate forcing is different for each glacier. For instance, De Angelis (2014) studied the sensitivity of mass balance to changes in the equilibrium-line altitude (ELA) using data from glaciers in the SPI. He showed that glacier hypsometry (characterized by the accumulation–area ratio (AAR)) has strong control on glacier variation in the SPI. According to studies in Greenland, Alaska and other regions (e.g. Joughin and others, 2004; Benn and others, 2007; Howat and others, 2007; Nick and others, 2009), calving also plays a critical role in glacier variation. Calving flux is controlled by glacier dynamics under the influence of physical conditions near the terminus (e.g. bed geometry, proglacial water depth, subglacial water pressure and basal sediments) (Van der Veen, 1996; Nick and others, 2009; Sugiyama and others, 2011). Melting of the calving front under the water is also a key component of calving glacier mass budget (Motyka and others, 2003; Rignot and others, 2010; Bartholomaus and others, 2013), whose magnitude is controlled by water temperature, salinity and circulation in front of a glacier. All these processes influence the response of calving glaciers to changes in climatic conditions, which results in the non-uniform glacier variations observed in Patagonia.

GPM and Glacier Ameghino (GA) are freshwater calving glaciers located in the southeast SPI (Fig. 1). They are in contact in the accumulation area, and the lower reaches are separated by 8 km. Despite their proximity, these two glaciers have shown contrasting fluctuations in recent decades, as noted by Nichols and Miller (1952) and Warren (1994). The terminus position of GPM has been stable (±500 m) since 1920, whereas GA has retreated by 4.2 km from 1928 to 1993, similar to most of the other calving glaciers in Patagonia (Warren, 1994; Aniya and others, 1997; Skvarca and Naruse, 1997). Thus, these two glaciers provide a unique opportunity to study key processes controlling the non-uniform response of calving glaciers to similar climate

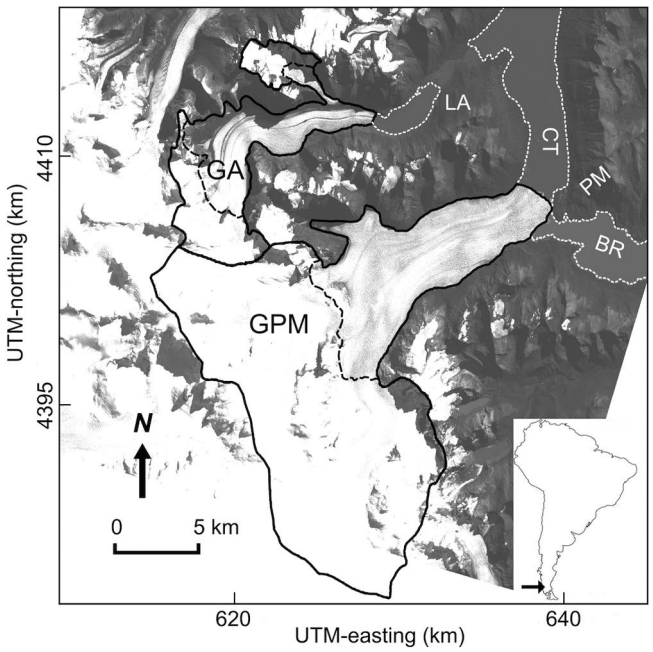

Fig. 1. Satellite image of GPM and GA, taken by ALOS/PRISM on 29 March 2008. Glacier margins and coastlines are indicated by the bold and dotted curves, respectively. The dashed lines indicate the ELA in 1999/2000 (after Stuefer and others, 2007). LA: Laguna Ameghino; CT: Canal de los Tempanos; PM: Peninsula Magallanes; and BR: Brazo Rico. Coordinates are UTM zone 18S. The inset shows the location of the study site in South America.

conditions. Previous studies propose the effect of the bed geometry near the terminus (Naruse and others, 1995) and valley shape (Aniya and Sato, 1995) on ice flow is the cause of the difference in glacier variations. In addition to the geometry near the terminus, Stuefer and others (2007) suggested that differences in AAR contribute to different responses under the same climate. Here we examine this hypothesis by examining the magnitude of the components of mass balance (accumulation, ablation and calving) for GPM and GA. We also extend the record of changes in surface elevation and terminus position for the two glaciers.

Recent advances in satellite remote-sensing techniques enable us to examine glacier variation patterns in detail. In particular, changes in surface elevation can be measured by comparing high-resolution digital elevation models (DEMs) obtained by satellite measurements and/or photogrammetric analysis of satellite images. In this study, we use satellite data to measure frontal positions and surface elevations in GPM and GA. The results are utilized to quantify recent frontal variations and ice thickness change. To investigate processes driving the different glacier variations, we perform mass-balance calculations and hypsometry analysis based on data obtained in this work as well as those reported in previous studies.

2. STUDY SITES

2.1. Glaciar Perito Moreno

GPM (50.5° S, 73.2° W) covers an area of 259 km^2 (Fig. 1; De Angelis, 2014). The glacier calves into two lakes, Brazo Rico and Canal de los Tempanos, which are part of Lago Argentino. The lake level is 185 m a.s.l. (Rott and others, 2005). The mean AAR from 2002 to 2004 is reported as 0.70 (ELA = 1230 ± 40 m a.s.l.) based on analysis of Moderate Resolution Imaging Spectroradiometer (MODIS) images (De Angelis, 2014). Based on field observations, Stuefer and others (2007) calculated surface mass balance in 1999/2000 and found the ELA to be 1170 m a.s.l.

GPM has shown only small terminus variations since 1920 compared to the other glaciers in Patagonia. Small variations that do occur are associated with the formation and collapse of an ice dam at the glacier front. Brazo Rico is often dammed by ice advancing onto Peninsula Magallanes (Fig. 1). Damming events have been observed repeatedly since the 1930s with intervals of a few years (Skvarca and Naruse, 1997), but the occurrence is irregular. Since 1999 three events have been reported: September 2003–March 2004 (Skvarca and Naruse, 2006), August 2005–March 2006 (Stuefer and others, 2007) and December 2007–July 2008; the outburst in July 2008 was the first observation of the ice-dam collapse in winter (Pasquini and Depetris, 2011).

2.2. Glaciar Ameghino

GA (50.45° S, 73.3° W) covers an area of 76 km^2 (Fig. 1). The mean AAR between 2002 and 2004 was 0.55 and ELA = 940 ± 40 m a.s.l. (De Angelis, 2014). GA now calves into Laguna Ameghino, which formed in 1967 as a result of glacier retreat. The lake, which is separated from Lago Argentino by 3 km, is 201 m a.s.l. (Aniya and Sato, 1995). After 1967, GA retreated rapidly for the next 9 years at a mean rate of 334 m a^{-1} (Warren, 1994). The rate decreased to 20 m a^{-1} between 1976 and 1986, and the glacier continued to retreat, similar to many other glaciers in Patagonia. The surface velocity of GA is smaller than that of GPM, because the glacier is thinner and narrower. The surface velocity at the calving front was 0.79 m a^{-1} in 1994, and a similar velocity was measured from satellite data in 2008 (Floricioiu and others, 2008).

3. METHODS

3.1. Surface elevation

Change in glacier surface elevation from February 2000 to 29 March 2008 was measured by differencing a DEM from the Shuttle Radar Topography Mission (SRTM) in February 2000 and a DEM produced from a stereo pair of satellite images obtained on 29 March 2008 by Panchromatic Remote-sensing Instruments for Stereo Mapping (PRISM) mounted on the Japanese Advanced Land Observation Satellite (ALOS). The horizontal resolution of the image was 2.5 m. The nadir- and forward-looking images with a processing level of 1B2 (geometrically corrected data) were distributed with rational polynomial coefficient (RPC) files by the Remote Sensing Technology Center (RESTEC) of Japan. Root-mean-square errors (RMSEs) of ALOS PRISM RPC were typically 1–5 m. We processed the stereo pair images for surface elevation with the aid of the Leica Photogrammetric Suite (LPS) in the ERDAS IMAGINE (Intergraph Co.) workstation. Surface elevation was measured by referring to stereoscopic three-dimensional images by LPS at gridpoints of the SRTM DEM as described below. The generated DEMs cover 35% and 75% of the total areas of GPM and GA, respectively. We were not able to generate DEMs in the accumulation areas because no visual contrast was available over snow-covered regions and dark shadow regions. The maximum error in DEMs produced by the same method is reported as ±4 m (Lamsal and others, 2011).

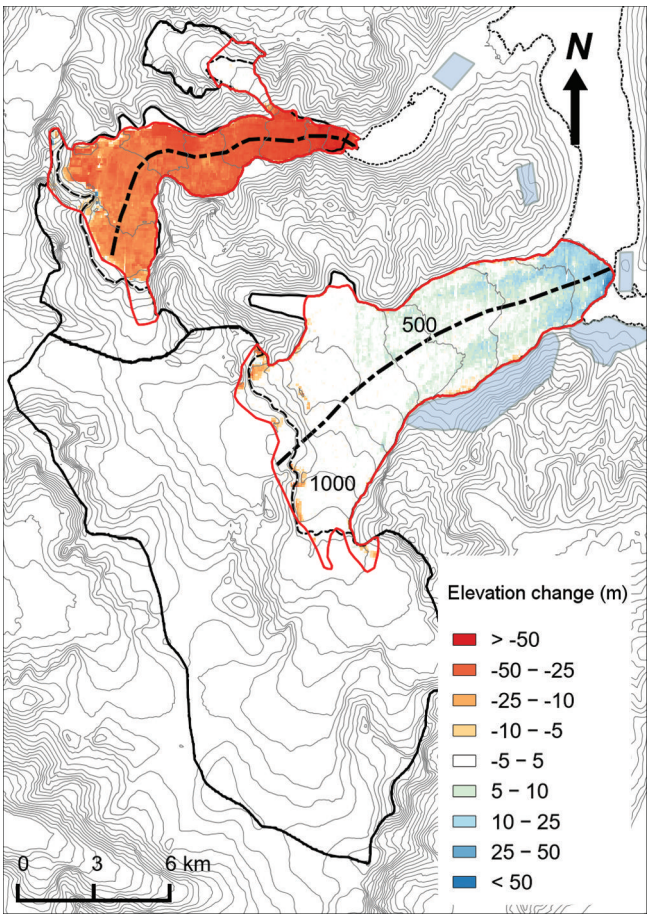

Fig. 2. Surface-elevation changes over GPM and GA from 2000 to 2008. Glacier margins and analyzed areas are indicated by the bold black and red curves. Contour intervals are 100 m. Dash-dotted curves indicate the central flowlines used in Figure 3. The dashed lines indicate the ELA in 1999/2000 (after Stuefer and others, 2007). Accuracy of the DEM differentiation was evaluated in the light-blue areas.

In addition to the ALOS DEM, we used a DEM generated by interferometric synthetic aperture radar (InSAR) measurement of the SRTM during 11 days in February 2000. We used SRTM v2.1 data with absolute accuracies in the horizontal and vertical directions of 20 and 16 m, respectively (Farr and others, 2007). The resolution of the SRTM DEM, after a projection on the area of study, was 73 m.

The DEMs were compared at gridpoints of the SRTM DEM to measure glacier surface elevation change from 2000 and 2008. Error in the measured elevation change was evaluated from changes obtained outside of the glaciers, where elevation change should be zero. This error evaluation was performed on different types of terrain near GPM and GA over an area of 3.1 km^2 and an elevation range of 187–1489 m a.s.l. indicated by light blue areas in Figure 2. The error is estimated to be ±2.4 m from the RMSE.

3.2. Terminus position

We measured the terminus displacement of GPM and GA from January 1999 to October 2012, using orthorectified Landsat 7 Enhanced Thematic Mapper Plus (ETM+) band 8 and Landsat 5 Thematic Mapper (TM) band 3 (provided by the US Geological Survey at http://earthexplorer.usgs.gov/). Frontal margins of the glaciers were delineated by visual

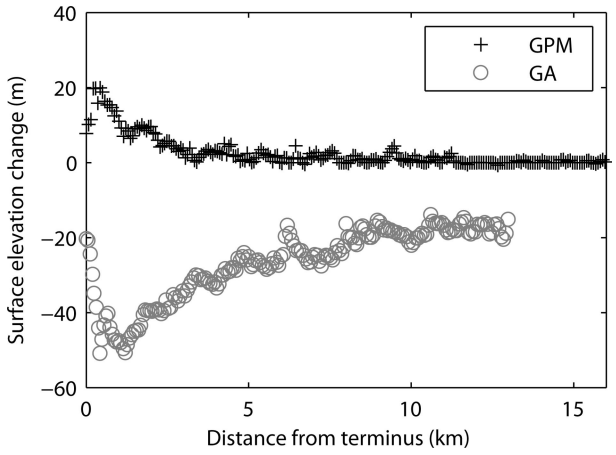

Fig. 3. Surface elevation change in GPM and GA along the central flowlines indicated in Figure 2.

observations on a computer screen, using geographical information system software ArcGIS (ESRI, Inc.). The accuracy of this procedure was equal to the image resolutions, which were 15 and 30 m for Landsat 7 and 5 images, respectively. Changes in the terminus positions were calculated by dividing the changes in ice surface area by the width of the calving front (Moon and Joughin, 2008).

4. RESULTS

4.1. Surface elevation

Surface-elevation changes were significantly different at GPM and GA. Results show ice thickening in GPM within 5 km of the terminus (Figs 2 and 3). The elevation change within this region was 10–30 m over the 8 years, which is equivalent to an ice volume increase of $0.25 \pm 0.19\,km^3$. Mean rate of elevation change over the studied 78 km^2 was $0.4 \pm 0.3\,m\,a^{-1}$. During this period, the glacier advanced by 230 m.

In contrast, GA showed surface lowering during the same period (Figs 2 and 3). The elevation change was more significant in the lower reaches, and the maximum change of –51 m ($-6.4\,m\,a^{-1}$) was observed at 410 m from the terminus in 2000 (Fig. 3). The mean changing rate over the 40 km^2 covered by the ALOS DEM was $-2.6 \pm 0.3\,m\,a^{-1}$. This surface lowering is equivalent to an ice volume loss of $0.83 \pm 0.09\,km^3$.

4.2. Terminus position

Figure 4 shows variations in the terminus positions of GPM and GA from January 1999 to October 2012. GPM repeated relatively small advances and retreats, resulting in the total displacement of +30 m over the study period. The range of the variation was 270 m. The long-term variation was small, but the data show clear seasonal variations with a mean amplitude of 123 m. The glacier retreated primarily from January to June, and then advanced for the rest of the year. The mean rate of retreat from January to June was $293\,m\,a^{-1}$, whereas the rate of advance was $210\,m\,a^{-1}$.

The total retreat of GA from 1999 to 2012 was 720 m, with a mean rate of $56\,m\,a^{-1}$ (Fig. 4). GA showed seasonal variations similar to GPM between 1999 and 2001, but it progressively retreated without a clear seasonal signal after

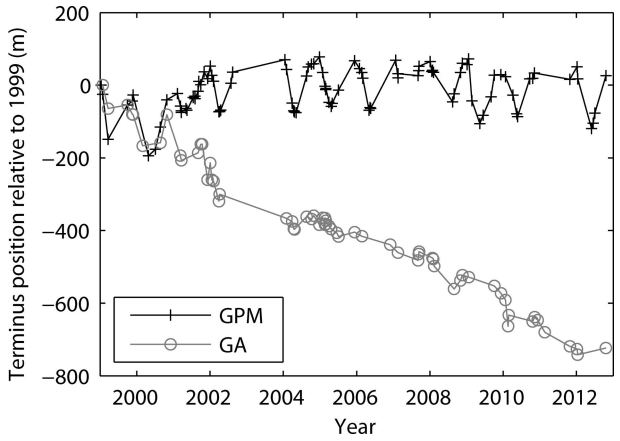

Fig. 4. Changes in the terminus positions relative to 1999 in GPM and GA. A negative value indicates terminus retreat.

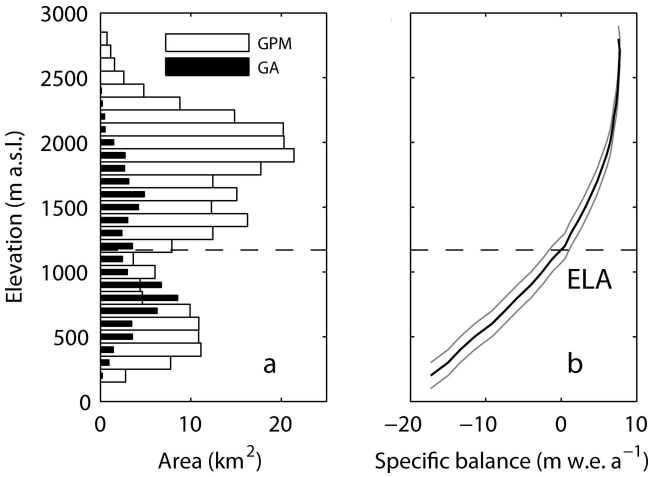

Fig. 5. (a) Hypsometries for GPM and GA with elevation intervals of 100 m. (b) Mass-balance profile for 1999/2000 (after Stuefer and others, 2007) (bold). Gray thin lines are mass-balance profiles for changes in ELA by ±100 m, which are used for the sensitivity experiments.

2001. According to previous studies, GA retreated at a rate of 334 m a^{-1} between 1967 and 1976, and the rate then declined to 20 m a^{-1} between 1976 and 1986 (Warren, 1994). The rate of retreat between 1999 and 2012 is 36% greater than that between 1976 and 1986, which is similar to those reported for other calving glaciers in the SPI from 1944/45 to 2005 (Masiokas and others, 2009; Lopez and others, 2010).

4.3. Glacier-wide mass balance

Glacier-wide mass balance of a calving glacier is

$$\Delta M \approx C_{\mathrm{sfc}} + A_{\mathrm{sfc}} - D = \int_{S_{\mathrm{c}}} b(z)\,\mathrm{d}S + \int_{S_{\mathrm{a}}} b(z)\,\mathrm{d}S - u_{\mathrm{D}} W H_{\mathrm{i}} \quad (1)$$

where C_{sfc} and A_{sfc} are the surface mass balance over the accumulation area S_{c} and in the ablation area S_{a}, and D is the calving flux (Cuffey and Paterson, 2010; Cogley and others, 2011). Surface mass balance at elevation z is given by $b(z)$ and integrated over the surface area S. Calving speed, glacier width and ice thickness at the calving front are denoted by u_{D}, W and H_{i} respectively. We evaluate the three components in the glacier-wide mass-balance Eqn (1) to investigate the driving mechanism of the mass changes in GPM and GA. Net surface mass balance above and below the ELA were computed using the elevation-dependent mass-balance profile reported for GPM by Stuefer and others (2007). To integrate the mass balance over the accumulation and ablation areas, we used hypsometry derived by the SRTM DEM in 2000 (Fig. 5a). The calving flux D in GPM was taken from the value estimated in Stuefer and others (2007), and that for GA was calculated from ice thickness (Warren and Aniya, 1999), flow speed near the terminus (Floricioiu and others, 2008) and terminus position changes obtained in this study.

Table 1 shows the glacier-wide mass balance and its components computed for GPM and GA for the 1999/2000 balance year. The glacier-wide mass balance is –0.1 ± 0.3 and –0.19 ± 0.05 km^3 w.e. a^{-1} for GPM and GA, respectively. These mass changes are equivalent to mean surface elevation changes of –0.4 ± 1.2 and –2.8 ± 1.2 m w.e. a^{-1}. Slightly negative mass change for GPM is consistent with the mean elevation change calculated by differencing DEMs over the period 2000–08 (0.4 ± 0.3 m w.e. a^{-1}) within the accuracy of the calculation, and the mass loss for GA agrees with the value from the DEMs (–2.6 ± 0.3 m w.e. a^{-1}) within the uncertainty. The computed mass balance for GA is more negative than the value estimated for 1995–2003 by Stuefer and others (2007) (–0.90 m w.e. a^{-1}). It is likely that the difference is a result of the different surface area and different AAR used in that study. Here we assume that our mass-balance calculation is sufficiently accurate to discuss processes controlling the mass change of the glaciers.

Table 1. Glacier-wide mass balance (ΔM), surface mass balance integrated over the accumulation area (C_{sfc}) and ablation area (A_{sfc}) and calving flux (D). C_{sfc} and A_{sfc} were calculated from the hypsometry (Fig. 5a) and the mass-balance profile reported by Stuefer and others (2007) for the 1999/2000 balance year (Fig. 5b). D for GPM is after Stuefer and others (2007) whereas D for GA was calculated in this study. Also indicated are glacier-wide specific mass balance ($\Delta M/S$) and the rate of surface elevation change measured by the DEM differentiation (Δh). The rate of elevation change represents the mean from 2000 to 2008 over the area analyzed in this study (Fig. 2)

	ΔM	C_{sfc}	A_{sfc}	D	$A_{\mathrm{sfc}}/(A_{\mathrm{sfc}}-D)$	$\lvert A_{\mathrm{sfc}}/C_{\mathrm{sfc}}\rvert$	$\Delta M/S$	Δh
	km^3 w.e. a^{-1}	km^3 w.e. a^{-1}	km^3 w.e. a^{-1}	km^3 w.e. a^{-1}			m w.e. a^{-1}	m w.e. a^{-1}
GPM	–0.10 ± 0.3	0.96 ± 0.18	–0.694 ± 0.07	0.361 ± 0.04	0.66	0.72	–0.4 ± 1.2	0.4 ± 0.3
GA	–0.19 ± 0.05	0.11 ± 0.03	–0.250 ± 0.04	0.046 ± 0.003	0.84	2.27	–2.8 ± 1.2	–2.6 ± 0.3
GA/GPM		0.11	0.36	0.13				

Table 2. Glacier-wide specific surface mass balance $(C_{sfc} + A_{sfc})/S$ and AAR calculated for the ELA reported for 1999/2000 (1170 m a.s.l.) (Stuefer and others, 2007) and those after changes by ±100 m

	GPM		GA	
ELA	$(C_{sfc} + A_{sfc})/S$	AAR	$(C_{sfc} + A_{sfc})/S$	AAR
m a.s.l.	m w.e. a^{-1}		m w.e. a^{-1}	
1170 + 100	0.2	0.70	–3.5	0.39
1170	1.0	0.73	–2.1	0.45
1170 – 100	1.9	0.74	–0.8	0.48

5. DISCUSSION

5.1. Drivers of contrasting glacier variations

The changes in surface elevation (Figs 2 and 3) and terminus position (Fig. 4) indicate significantly different variations in GPM and GA. While GPM showed little change in terminus position and surface elevation, GA rapidly retreated and thinned during the study period. Below, we discuss the mechanism for the contrasting variations of these two glaciers by partitioning the mass balance into components (Table 1).

The three components of the mass-balance equation (C_{sfc}, A_{sfc} and D) in GA are smaller than those in GPM (Table 1) because GA is substantially smaller in dimension. Surface mass balance in the accumulation area (C_{sfc}) and calving flux (D) in GA are 11% and 13% respectively of those in GPM. Surface mass balance in the ablation area in GA is 36% of that in GPM, which is significantly greater than the other two components. Furthermore, the fraction of the negative mass balance in the ablation area to the total ablation $A_{sfc}/(A_{sfc} - D)$ is 0.84 in GA, greater than the fraction in GPM (0.66). The fraction of surface mass balance in the accumulation and ablation areas ($|A_{sfc}/C_{sfc}|$) is greater in GA (2.27) than in GPM (0.72). These values indicate a relatively greater contribution of negative surface mass balance over the ablation area in the glacier-wide mass balance in GA. This analysis also suggests that A_{sfc} is the primary reason for the contrasting response of GA and GPM despite similar climate conditions.

The contrasting mass-balance regimes of the two glaciers are affected by the AAR. The accumulation area of GA is very steep and small compared to the flat ablation area extending in the lower elevation area (Figs 2 and 5a). In contrast, GPM has a relatively flat and large accumulation area (Figs 2 and 5a). If we apply the ELA reported for GPM in 1999/2000 (1170 m a.s.l.; Stuefer and others, 2007) to the SRTM DEM, accumulation and ablation areas are 36.5 and 29.4 km^2 (AAR = 0.45) for GA, and 190.6 and 72.1 km^2 (AAR = 0.73) for GPM (Fig. 5a).

The mean AAR over the major calving glaciers in the SPI is 0.71 based on the AARs reported by De Angelis (2014) and for the glaciers listed in Aniya and others (1997). The AAR of GA (0.45) is substantially smaller than the mean over the SPI, which resulted in the rapid retreat and thinning of this glacier. The AAR is small in GA because a large surface area is distributed slightly below the ELA (940 m a.s.l.) (De Angelis, 2014). 28% of the surface area is at 800–1000 m a.s.l. (Fig. 5a), which suggests that AAR is sensitive to recent increase in ELA. To investigate the sensitivity of mass balance to changes in ELA, we calculated surface accumulation and ablation based on the mass-balance profile reported by Stuefer and others (2007) (Fig. 5b). We kept calving flux constant in this experiment. When ELA is elevated by 100 m (Fig. 5b), the specific surface mass balance of GA decreases from –2.1 m w.e. a^{-1} to –3.5 m w.e. a^{-1} (Table 2). Mass balance of GPM also decreases (from 1.0 m w.e. a^{-1} to 0.2 m w.e. a^{-1}), but the magnitude of the change is smaller. It is likely that the AAR plays a critical role in the greater sensitivity of GA because the decrease in AAR is greater (from 0.45 to 0.39) than for GPM (0.73 to 0.70). Mass balance and AAR of GA are also more sensitive to lowering ELA (–100 m). Results indicate that GA is more sensitive to climate forcing because of the characteristic surface area distribution (Fig. 5a).

Calving glaciers are expected to advance, irrespective of climatic forcing, when AAR exceeds 0.8 (Post and others, 2011). The AAR of GPM is similar to this number, thus explaining the stability of this glacier. The AAR of GPM (0.73) is slightly larger than the mean for SPI (0.71; De Angelis, 2014), probably because of the geometry of the terminus region. Since GPM calves into two lakes, further advance was difficult in the past, and AAR has remained relatively constant and large. This is a plausible reason why GPM has shown no significant retreat compared to GA and other retreating glaciers in Patagonia.

5.2. Glacier fate

We believe that GA will continue to retreat in the future, because accumulation is not sufficient to counterbalance melting in the large ablation area. If we assume the surface mass balance and ELA in 1999/2000 (Stuefer and others, 2007), surface mass balance in the accumulation and ablation areas (C_{sfc} and A_{sfc}) balance when the terminus retreats to 700–800 m a.s.l. It takes ~100 years to reach this condition under the retreat rate observed for 1999–2012 (56 m a^{-1}). In fact, further retreat is necessary to reach the steady state because the accumulation area shrinks as the glacier thins and the surface lowers. We neglect calving flux (D) in the calculation because it currently accounts for only 20% of the total ablation and will likely decrease as the terminus retreats from the lake. Further, Rasmussen and others (2007) discussed the importance of transition from solid to liquid precipitation under a warming climate. Because of the large area at low elevations, GA is more sensitive to such influence of temperature rise on snow accumulation.

Immediate change is not likely at GPM because AAR is large and the glacier has been stable for a long time in this geometry. Indeed, GPM thickened near the terminus in 2000–08 (Fig. 3). Presumably, ice is thickening in this region because the glacier is buttressed by Peninsula Magallanes. This hypothesis is supported by the fact that three damming events occurred between 2000 and 2008, whereas no event occurred in the 1990s (Stuefer and others, 2007). Our analysis demonstrates that contribution of the calving flux to the total ablation is relatively large (36%; Table 1), and thus glacier dynamics near the terminus may play a key role in future glacier change. Once the glacier accelerates, as has been observed in other calving glaciers in the SPI (Rivera and others, 2012; Sakakibara and others, 2013; Sakakibara and Sugiyama, 2014), mass that is currently balanced would be altered in a way that causes the glacier to thin and retreat. Such a change can be triggered by meltwater increase and

thinning of the glacier, because ice speed in the lower reaches of GPM is very sensitive to the effective pressure, i.e. ice overburden pressure minus subglacial water pressure (Sugiyama and others, 2011). Thus, glacier dynamics should be carefully monitored to predict a rapid change of GPM in the future.

6. CONCLUSIONS

We studied recent variations in GPM and GA in the SPI, and discussed the drivers of contrasting response of these two glaciers under similar climatic conditions. We measured surface elevation changes by comparing the SRTM DEM in 2000 and ALOS DEM in 2008 generated in this study. Changes in terminus positions were analyzed from 1999 and 2012 with Landsat 5 and 7 images. The results indicated significantly different variations in GPM and GA. Only small changes occurred both in the surface elevation ($+0.4\ \mathrm{m\ a^{-1}}$ over the lower 35% area) and the terminus position (+26 m from 1999 to 2012) in GPM. In contrast, the surface lowered at a rate of $2.6\ \mathrm{m\ a^{-1}}$ from 2000 to 2008 over the lower 75% area in GA, and total retreat from 1999 to 2012 was 723 m. Three components of the glacier-wide mass balance were computed to investigate the contrasting glacier variations. GA has a large mass loss in the ablation area, which exerts strong control on the glacier-wide mass balance. These mass-balance regimes are due to the small AAR (0.45) in GA compared to that in GPM (0.73). Sensitivity experiments indicated that mass balance and AAR of GA are more sensitive to changes in ELA. We conclude that GA is rapidly retreating and thinning under the influence of melting over the large ablation area, whereas GPM is stable at the current geometry since AAR is large enough to maintain the glacier-wide mass balance. The result is consistent with previous studies of these two glaciers (e.g. Stuefer and others, 2007). Our analysis confirms an important role of AAR in the glacier retreat and thinning in Patagonia (e.g. De Angelis, 2014) and suggests possible use of this parameter for predicting the future of glaciers in Patagonia.

ACKNOWLEDGEMENTS

SRTM v2.1 and v4.1 are downloaded from http://eros.usgs.gov/ and http://www.cgiar-cs.org/, respectively. We thank P. Skvarca for helpful discussion. This research was supported by the Japan Society for the Promotion of Science, Grants-in-Aid for Scientific Research B 23403006. We thank Hernán De Angelis, an anonymous reviewer and the Scientific Editor G. Leysinger Vieli for help in improving the manuscript.

REFERENCES

Aniya M (1999) Recent glacier variations of the Hielo Patagónicos, South America, and their contribution to sea-level change. *Arct. Antarct. Alp. Res.*, **31**(2), 165–173

Aniya M and Sato H (1995) Morphology of Ameghino Glacier and landforms of Ameghino Valley, southern Patagonia. *Bull. Glacier Res.*, **13**, 69–82

Aniya M, Sato H, Naruse R, Skvarca P and Casassa G (1997) Recent glacier variations in the Southern Patagonia Icefield, South America. *Arct. Alp. Res.*, **29**(1), 1–12

Bartholomaus TC, Larsen CF and O'Neel S (2013) Does calving matter? Evidence for significant submarine melt. *Earth Planet. Sci. Lett.*, **380**, 21–30 (doi: 10.1016/j.epsl.2013.08.014)

Benn DI, Warren CW and Mottram RH (2007) Calving processes and the dynamics of calving glaciers. *Earth-Sci. Rev.*, **82**(3–4), 143–179 (doi: 10.1016/j.earscirev.2007.02.002)

Cogley JG and 10 others. (2011) *Glossary of glacier mass balance and related terms*. (IHP-VII Technical Documents in Hydrology 86) UNESCO–International Hydrological Programme, Paris

Cuffey KM and Paterson WSB (2010) *The physics of glaciers*, 4th edn. Butterworth-Heinemann, Oxford

Davies BJ and Glasser NF (2012) Accelerating shrinkage of Patagonian glaciers from the Little Ice Age (∼AD 1870) to 2011. *J. Glaciol.*, **58**(212), 1063–1084 (doi: 10.3189/2012JoG12J026)

De Angelis H (2014) Hypsometry and sensitivity of the mass balance to changes in equilibrium-line altitude: the case of the Southern Patagonia Icefield. *J. Glaciol.*, **60**(219), 14–28 (doi: 10.3189/2014JoG13J127)

Farr TG and 17 others (2007) The Shuttle Radar Topography Mission. *Rev. Geophys.*, **45**(2), RG2004 (doi: 10.1029/2005RG000183)

Floricioiu D, Eineder M, Rott H and Nagler T (2008) Velocities of major outlet glaciers of the Patagonia Icefield observed by TerraSAR-X. In *Proceedings of the International Geoscience and Remote Sensing Symposium (IGARSS 2008), 7–11 July 2008, Boston, MA, USA, Vol. 4*. Institute of Electrical and Electronics Engineers, Piscataway, NJ, 347–350

Howat IM, Joughin IR and Scambos TA (2007) Rapid changes in ice discharge from Greenland outlet glaciers. *Science*, **315**(5818), 1559–1561 (doi: 10.1126/science.1138478)

Joughin I, Abdalati W and Fahnestock MA (2004) Large fluctuations in speed on Greenland's Jakobshavn Isbræ glacier. *Nature*, **432**(7017), 608–610 (doi: 10.1038/nature03130)

Lamsal D, Sawagaki T and Watanabe T (2011) Digital terrain modelling using Corona and ALOS PRISM data to investigate the distal part of Imja Glacier, Khumbu Himal, Nepal. *J. Mt. Sci. [China]*, **8**(3), 390–402 (doi: 10.1007/s11629-011-2064-0) [in Chinese]

Lopez P, Chevallier P, Favier V, Pouyaud B, Ordenes F and Oerlemans J (2010) A regional view of fluctuations in glacier length in southern South America. *Global Planet. Change*, **71**(1–2), 85–108 (doi: 10.1016/j.gloplacha.2009.12.009)

Masiokas M, Rivera A, Espizua LE, Villalba R, Delgado S and Aravena JC (2009) Glacier fluctuations in extratropical South America during the past 1000 years. *Palaeogeogr., Palaeoclimatol., Palaeoecol.*, **281**(3–4), 242–268 (doi: 10.1016/j.palaeo.2009.08.006)

Meier MF and Post A (1987) Fast tidewater glaciers. *J. Geophys. Res.*, **92**(B9), 9051–9058 (doi: 10.1029/JB092iB09p09051)

Moon T and Joughin I (2008) Changes in ice front position on Greenland's outlet glaciers from 1992 to 2007. *J. Geophys. Res.*, **113**(F2), F02022 (doi: 10.1029/2007JF000927)

Motyka RJ, Hunter L, Echelmeyer KA and Connor C (2003) Submarine melting at the terminus of a temperate tidewater glacier, LeConte Glacier, Alaska, U.S.A. *Ann. Glaciol.*, **36**, 57–65 (doi: 10.3189/172756403781816374)

Muto M and Furuya M (2013) Surface velocities and ice-front positions of eight major glaciers in the Southern Patagonian Ice Field, South America, from 2002 to 2011. *Remote Sens. Environ.*, **139**, 50–59 (doi: 10.1016/j.rse.2013.07.034)

Naruse R, Aniya M, Skvarca P and Casassa G (1995) Recent variations of calving glaciers in Patagonia, South America, revealed by ground surveys, satellite-data analyses and numerical experiments. *Ann. Glaciol.*, **21**, 297–303

Nichols RL and Miller MM (1952) The Moreno Glacier, Lago Argentino, Patagonia: advancing glaciers and nearby simultaneously retreating glaciers. *J. Glaciol.*, **2**(11), 41–50/39

Nick FM, Vieli A, Howat IM and Joughin I (2009) Large-scale changes in Greenland outlet glacier dynamics triggered at the terminus. *Nature Geosci.*, **2**(2), 110–114 (doi: 10.1038/ngeo394)

Pasquini AI and Depetris PJ (2011) Southern Patagonia's Perito Moreno Glacier, Lake Argentino, and Santa Cruz River

hydrological system: an overview. *J. Hydrol.*, **405**(1–2), 48–56 (doi: 10.1016/j.jhydrol.2011.05.009)

Post A, O'Neel S, Motyka RJ and Streveler G (2011) A complex relationship between calving glaciers and climate. *Eos*, **97**(37), 305–306 (doi: 10.1029/2011EO370001)

Rasmussen LA, Conway H and Raymond CF (2007) Influence of upper air conditions on the Patagonia icefields. *Global Planet. Change*, **59**(1–4), 203–216 (doi: 10.1016/j.gloplacha.2006.11.025)

Rignot E, Rivera A and Casassa G (2003) Contribution of the Patagonian icefields of South America to sea level rise. *Science*, **302**(5644), 434–437 (doi: 10.1126/science.1087393)

Rignot E, Koppes M and Velicogna I (2010) Rapid submarine melting of the calving faces of West Greenland glaciers. *Nature Geosci.*, **3**(3), 187–191 (doi: 10.1038/ngeo765)

Rivera A, Benham T, Casassa G, Bamber J and Dowdeswell JA (2007) Ice elevation and areal changes of glaciers from the Northern Patagonia Icefield, Chile. *Global Planet. Change*, **59**(1–4), 126–137 (doi: 10.1016/j.gloplacha.2006.11.037)

Rivera A, Koppes M, Bravo C and Aravena JC (2012) Little Ice Age advance and retreat of Glaciar Jorge Montt, Chilean Patagonia. *Climate Past*, **8**(2), 403–414 (doi: 10.5194/cp-8-403-2012)

Rott H, Stuefer M, Nagler T and Riedl C (2005) Recent fluctuations and damming of Glaciar Perito Moreno, Patagonia, observed by means of ERS and Envisat imagery. In Lacoste H and Ouwehand L eds *Proceedings of the 2004 Envisat & ERS Symposium, 6–10 September 2004, Salzburg, Austria*. ESA Publications, Noordwijk

Sakakibara D and Sugiyama S (2014) Ice-front variations and speed changes of calving glaciers in the Southern Patagonia Icefield from 1984 to 2011. *J. Geophys. Res.*, **119**(11), 2541–2554 (doi: 10.1002/2014JF003148)

Sakakibara D, Sugiyama S, Sawagaki T, Marinsek S and Skvarca P (2013) Rapid retreat, acceleration and thinning of Glaciar Upsala, Southern Patagonia Icefield, initiated in 2008. *Ann. Glaciol.*, **54**(63 Pt 1), 131–138 (doi: 10.3189/2013AoG63A236)

Skvarca P and Naruse R (1997) Dynamic behavior of Glaciar Perito Moreno, southern Patagonia. *Ann. Glaciol.*, **24**, 268–271

Skvarca P and Naruse R (2006) Erratum. Overview of the ice-dam formation and collapse of Glaciar Perito Moreno, southern Patagonia, in 2003/04. *J. Glaciol.*, **178**(52), 476–478 (doi: 10.3189/172756506781828539)

Skvarca P, Marinsek S and Aniya M (2010) Documenting 23 years of areal loss of Hielo Patagónico Sur, recent climate data and potential impact on Río Santa Cruz water discharge. In *Abstracts. International Glaciological Conference. Ice and Climate Change: A View from the South*. Centro de Estudios Científicos, Valdivia, 82

Stuefer M, Rott H and Skvarca P (2007) Glaciar Perito Moreno, Patagonia: climate sensitivities and glacier characteristics preceding the 2003/04 and 2005/06 damming events. *J. Glaciol.*, **53**(180), 3–16 (doi: 10.3189/172756507781833848)

Sugiyama S and 7 others (2011) Ice speed of a calving glacier modulated by small fluctuations in basal water pressure. *Nature Geosci.*, **4**(9), 597–600 (doi: 10.1038/ngeo1218)

Van der Veen CJ (1996) Tidewater calving. *J. Glaciol.*, **42**(141), 375–385

Warren CR (1994) Freshwater calving and anomalous glacier oscillations: recent behaviour of Moreno and Ameghino Glaciers, Patagonia. *Holocene*, **4**(4), 422–429 (doi: 10.1177/095968369400400410)

Warren C and Aniya M (1999) The calving glaciers of southern South America. *Global Planet. Change*, **22**(1–4), 59–77

Willis MJ, Melkonian AK, Pritchard ME and Rivera A (2012) Ice loss from the Southern Patagonian Ice Field, South America, between 2000 and 2012. *Geophys. Res. Lett.*, **39**(17), L17501 (doi: 10.1029/2012GL053136)